Molecular Cell, Vol. 19, 259–269, July 22, 2005, Copyright ©2005 by Elsevier Inc. DOI 10.1016/j.molcel.2005.06.006

Crystal Structure of Bacteriophage λcII and Its DNA Complex

Deepti Jain,[1] Youngchang Kim,[2] Karen L. Maxwell,[3] Steven Beasley,[3] Rongguang Zhang,[2] Gary N. Gussin,[4] Aled M. Edwards,[3] and Seth A. Darst[1,*]

[1]The Rockefeller University
1230 York Avenue
New York, New York 10021
[2]Biosciences Division
Structural Biology Center
Argonne National Laboratory
9700 South Cass Avenue
Argonne, Illinois 60439
[3]Ontario Center for Structural Proteomics
Banting and Best Department of Medical Research
University of Toronto
112 College Street
Toronto, Ontario M5G 1L6
Canada
[4]Department of Biological Sciences
University of Iowa
141 BB
Iowa City, Iowa 52242

Summary

The tetrameric cII protein from bacteriophage λ activates transcription from the phage promoters P_{RE}, P_I, and P_{AQ} by binding to two direct repeats that flank the promoter –35 element. Here, we present the X-ray crystal structure of cII alone (2.8 Å resolution) and in complex with its DNA operator from P_{RE} (1.7 Å resolution). The structures provide a basis for modeling of the activation complex with the RNA polymerase holoenzyme, and point to the key role for the RNA polymerase α subunit C-terminal domain (αCTD) in cII-dependent activation, which forms a bridge of protein/protein interactions between cII and the RNA polymerase σ subunit. The model makes specific predictions for protein/protein interactions between cII and αCTD, and between αCTD and σ, which are supported by previous genetic studies.

Introduction

The transcription activator protein cII of bacteriophage λ plays a key role in the switch that governs lytic or lysogenic phage development (Echols, 1986; Ho et al., 1986). Regulation of cII occurs at the levels of transcription, translation initiation, mRNA stability, and proteolysis. Conditions that stabilize cII favor the lysogenic response (Obuchowski et al., 1997b).

Although cII belongs to the helix-turn-helix (HTH) family of DNA binding proteins (Matthews et al., 1982; Pabo and Sauer, 1984), it is unusual in several respects. Activators of the HTH family (such as the λ repressor/activator cI; Beamer and Pabo, 1992; Jain et al., 2004) typically function as homodimers, and recognize DNA operators comprising an inverted repeat on the same face of the DNA duplex as the RNA polymerase (RNAP), facilitating direct protein/protein interactions with the RNAP α subunit C-terminal domain (αCTD) and/or the σ subunit (Dove et al., 2003; Hochschild and Dove, 1998). On the other hand, cII functions as a homotetramer of 97 amino acid monomers (11 kDa; Ho et al., 1982) and recognizes direct repeats of a tetranucleotide sequence ($TTGCN_6TTGC$) on the face of the DNA duplex opposite from the RNAP (Ho et al., 1983).

The direct repeats recognized by cII exactly straddle the promoter –35 element hexamer, making cII a class II activator (Ishihama, 1992). Class II activators bind operators that overlap with the –35 element, and in most cases make direct protein/protein contacts with σ domain 4 (σ_4; Campbell et al., 2002) bound at the –35 element. In the case of cII, however, there is no evidence for direct cII/σ_4 interactions.

The RNAP αCTDs play an important role in transcription initiation by making multipartite interactions with any or all of the following: Upstream promoter DNA, σ_4, and transcriptional activators (Busby and Ebright, 1999; Chen et al., 2003; Gourse et al., 2000; Ross et al., 2003). Deletion of αCTD, or αCTD point mutants, causes severe defects in cII-dependent activation of the λ promoter P_{RE} (Gussin et al., 1992; Kedzierska et al., 2004; Marr et al., 2004; Obuchowski et al., 1997a; Wegrzyn et al., 1992), and interactions of αCTD with DNA just upstream of the –35 element are critical for full activation (Kedzierska et al., 2004). With many class II activators, one or both αCTDs bind immediately upstream of the activator on the same face of the DNA double helix, and make protein/protein interactions with the activator.

Because of its unusual nature, many aspects of cII function remain mysterious. How does the tetrameric cII interact with its DNA operator? How does cII activate transcription while binding to the opposite face of the DNA duplex as the RNAP? Here, we present crystal structures of λcII alone and in complex with its DNA operator. These structures, combined with modeling as well as previous genetic and biochemical results, provide insights that help answer many of these questions.

Results and Discussion

Crystallization and Structure Determination of λcII and the λcII/DNA Complex

We performed crystallization trials with full-length λcII protein (residues 1–97) combined with DNA fragments corresponding to the –35 region of the P_{RE} promoter, containing the cII-specific direct repeats and the intervening P_{RE} –35 element (Figure 1A). Crystals were obtained under a variety of conditions, but diffraction never extended beyond 5 Å resolution.

The cII protein has a very short half-life in vivo because it is a target of the proccesive, ATP-dependent FtsH (HflB) protease (Karata et al., 1999). The C-ter-

*Correspondence: darst@rockefeller.edu

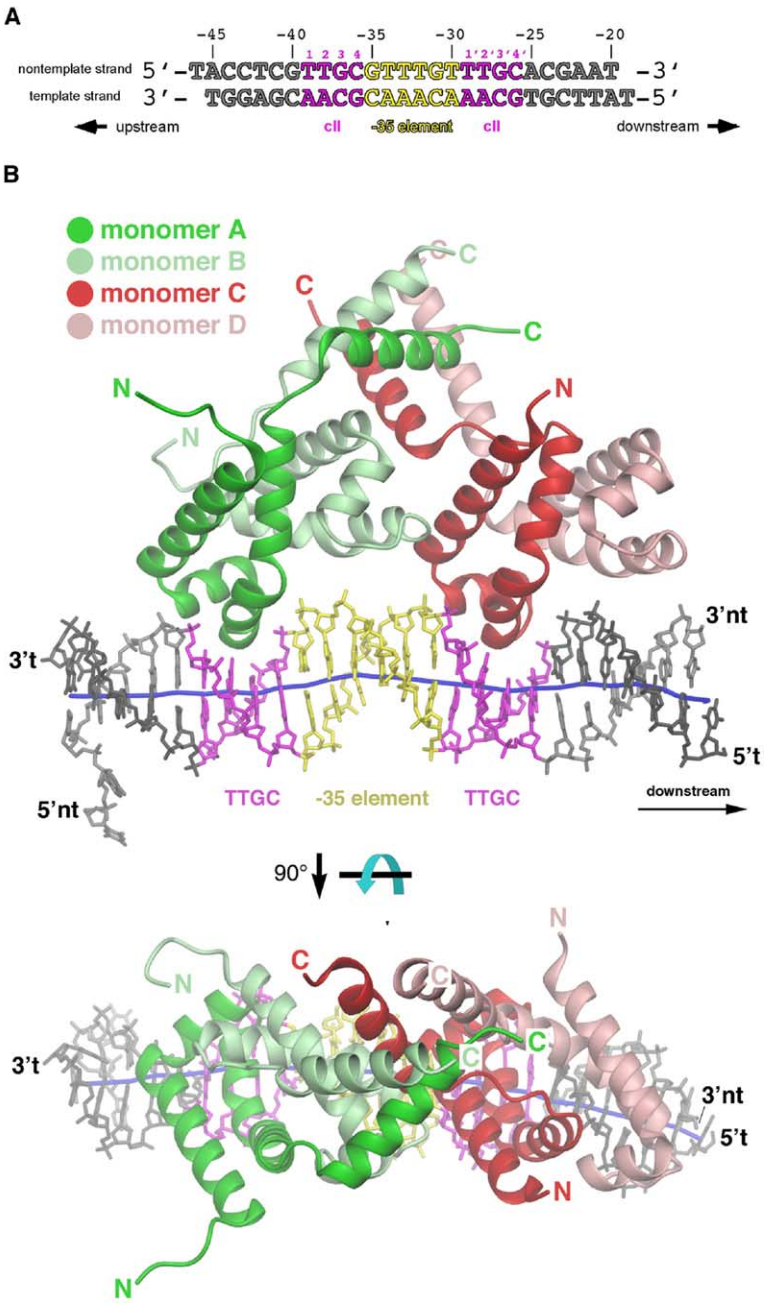

Figure 1. Structural Overview of the λcII/DNA Complex

(A) Synthetic 27-mer oligonucleotides used for crystallization. The black numbers above the sequence denote the DNA position with respect to the transcription start site at +1 for P_{RE}. The −35 element is colored yellow. The λcII-specific direct repeats are magenta, with the upstream repeat labeled 1–4, and the downstream repeat 1′–4′.

(B) Two views of the λcII/DNA complex related by a 90° rotation about the horizontal axis as shown. Proteins are shown as α carbon backbone ribbons with λcII monomer A (λcIIA) colored dark green; λcIIB, light green; λcIIC, dark red; and λcIID, pink. The DNA is color coded as in (A). The template (t) and nontemplate (nt) strands are denoted.

minal tail of cII, roughly residues 85–97 ($cII^{85–97}$), is unstructured and highly flexible (Datta et al., 2005), and the same region is sufficient as a recognition signal for FtsH (Kobiler et al., 2002). In vivo and in vitro, this flexible C-terminal tail of cII is not needed for DNA binding or activation functions (Datta et al., 2005; Kobiler et al., 2002). Therefore, we used limited proteolysis experiments in the presence of DNA (data not shown) to identify a stable fragment corresponding to $cII^{4–82}$ that retains the DNA binding properties (also see Datta et al., 2005). This construct would also be expected to retain activation functions (Datta et al., 2005; Kobiler et al., 2002).

The $cII^{4–82}$ fragment and a 27 bp DNA fragment containing the −35 region of the P_{RE} promoter (Figure 1A) were crystallized by vapor diffusion (see Experimental Procedures). The structure, determined by mutliwavelength anomalous dispersion (Hendrickson, 1991) using crystals containing selenomethionyl-substituted λcII, was refined to an R/R_{free} of 20.9/22.8 at 1.7 Å resolution (Table 1; Figure S1 in the Supplemental Data available with this article online).

In addition, full-length λcII alone was crystallized by vapor diffusion (see Experimental Procedures). The crystals diffracted to 2.8 Å. The structure was solved by a combination of molecular replacement (using a cII pro-

Table 1. Crystallographic Analysis

Diffraction Data								
Data Set	Wavelength (Å)	Resolution (Å)	Number of Reflections (Total/Unique)	Completeness (%)	$I/\sigma(I)$	R_{sym}[a] (%)	Number of Sites	Phasing Power[b]
SeMet(λ1)[c,d] cII^{4-82}/DNA	0.97903	20–2.25 (2.33–2.25)	134,381/45,507	98.4(92.8)	14.2 (4.3)	5.1 (23.1)	12	1.35
SeMet(λ2)[c,d] cII^{4-82}/DNA	0.97922	20–2.25 (2.33–2.25)	95,816/45,116	98.7(94.0)	14.3 (3.5)	4.3 (21.1)	12	1.29
SeMet(λ3)[c,d] cII^{4-82}/DNA	0.96384	20–2.25 (2.33–2.25)	97,619/45,701	98.9(98.1)	11.6 (2.6)	5.1 (27.2)	12	1.14
Native[d] cII^{4-82}/DNA	0.98396	50–1.7 (1.76–1.7)	305,549/59,978	97.3(99.9)	8.7 (2.1)	6.7 (60.9)		
SeMet(λ1)[c,e] cII	0.97926	50–3.2 (3.31–3.2)	65,405/11,276	99.0(98.9)	11.3 (3.9)	7.7 (31.3)	12	
Native[e,f] cII	0.97926	50–2.6 (2.69–2.6)	70,744/11,571	96.5(96.5)	8.9 (1.2)	4.8 (59.0)		

Refinement (Against Native Data Sets)	cII^{4-82}/DNA	cII
Resolution (Å)	50–1.7	50–2.8
Number of solvent molecules	417	88
R_{cryst}/R_{free}[g] (%)	20.9/22.8	25.5/28.6
Rmsd bond lengths	0.019	0.028
Rmsd bond angles	1.864	2.38

cII^{4-82}/DNA space group, $P2_1$; unit cell, a = 44.771 Å, b = 97.132 Å, c = 59.869 Å, β = 105.363°; cII space group, $C222_1$, unit cell, a = 59.557 Å, b = 108.160 Å, c = 111.449 Å; Figure of merit: cII^{4-82}/DNA (20–2.3 Å resolution), 0.35, cII (50–3.5 Å resolution), 0.39.

[a] $R_{sym} = \Sigma|I - \langle I \rangle|/\Sigma I$, where I is observed intensity and $\langle I \rangle$ is average intensity obtained from multiple observations of symmetry related reflections.

[b] Phasing power and figure of merit as calculated by MLPHARE (Otwinowski, 1991) for cII-DNA and by SOLVE (Terwilliger and Berendzen, 1999) for cII alone.

[c] Scaling statistics for SeMet datasets calculated without combining anomalous pairs.

[d] The cII^{4-82}/DNA datasets were collected at the National Synchrotron Light Source Beamline X9A.

[e] The cII datasets were collected at the Advanced Photon Source Beamline SBC-19ID.

[f] The Native cII dataset was collected to 2.6 Å resolution, but the structure was refined to 2.8 Å resolution.

[g] $R_{cryst} = \Sigma||F_{observed}| - |F_{calculated}||/\Sigma|F_{observed}|$, $R_{free} = R_{cryst}$, calculated using 5% random data omitted from the refinement.

tein dimer from the structure of the DNA complex as a search model) and single anomalous dispersion, using a data set collected from selenomethionyl-substituted λcII.

Overall Structure

Crystal structures for both λcII alone (2.8 Å resolution) and the λcII/DNA complex (1.7 Å resolution) were determined. In the discussion and figures to follow, we focus on the cII/DNA complex because of the higher resolution and quality of the refinement (Table 1).

It is interesting to note that the cII/DNA complex packs in the crystal lattice in a very unusual manner. In the vast majority of protein/DNA complex crystals, the DNA contained zero (blunt-ended), one, or two complementary overhanging bases at the ends, producing pseudocontinuous DNA helices through the crystal by end-to-end packing of the DNA (see Tan et al., 2000). In the case of the cII/DNA complex, the DNA was designed with T overhangs (Figure 1A) to promote end-to-end DNA packing via Hoogstein base pairing. Nevertheless, there are no DNA/DNA interactions in the packing of the cII/DNA complex. Instead, both ends of the DNA fragment make intimate contacts with protein surfaces from symmetry-related protein molecules (Figures S2, S3, and S4). Remarkably, at the DNA upstream end, an AT Watson-Crick base pair is disrupted in order to facilitate contacts of the DNA with the protein surface (Figure S4).

As expected, the functional cII assembly is a tetramer (Ho et al., 1982). The cII monomer comprises four α helices (h1–4) arranged in two distinct structural elements (Figure 2), the N-terminal DNA binding domain (DBD; h1–3) and the C-terminal helix (h4).

The DBD comprises helices h1–3, which pack into a compact, globular domain. Each of the four DBDs of the cII tetramer are very similar in structure. Comparing residues 7–59, the root-mean-square deviations of α carbon positions ranging from 0.4 Å (comparing monomers A and C) to 1.7 Å (comparing monomers B and C). Helices h2 and h3 of each DBD form the predicted HTH motif (Ho et al., 1988). Helix h3, the recognition helix, contains an unusual 60° kink (between helices h3a and h3b, Figure 2) induced by a Pro residue at position 49. The Pro is conserved among cII-like proteins of several bacteriophages (1639, 434, 933H, HK620, and P22).

The individual DBDs pair into two sets of dimers, with monomer A dimerizing with B, and C with D (Figure 1B). That the cII tetramer comprises a dimer of dimers explains the finding that the Hill coefficient for activation in vitro is close to 2 (Shih and Gussin, 1984). Each dimer shows pseudo 2-fold symmetry, with an axis of rotation tilted roughly 45° with respect to the main axis of the DNA double helix. The two dimers (A/B and C/D) are

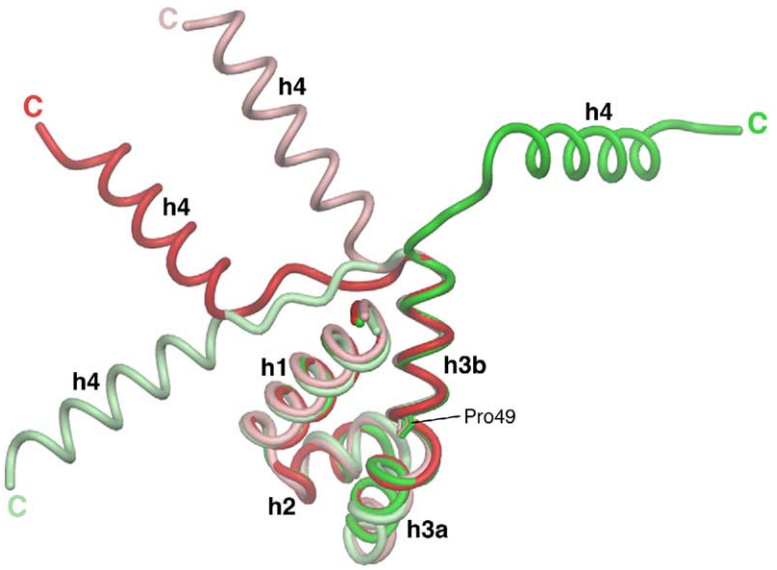

Figure 2. λcII Monomer Conformations

The λcII monomers, superimposed by their DBDs, are shown as α carbon backbone worms, color coded as in Figure 1. Helices h1, h2, h3a, and h3b of the DBD are labeled, along with the C-terminal h4. The side chain atoms for Pro49, which gives rise to the kink separating h3a and h3b, are also shown.

also very similar in structure—with an overall rmsd (comparing 106 α carbon positions) of 1.1 Å. The dimer interface is extensive (average buried surface area of 1738 $Å^2$ for the DBDs) and almost exclusively hydrophobic.

Although four monomers form the cII tetramer, they do not assemble into a 4-fold symmetrical arrangement. Rather, the A/B dimer is related to the C/D dimer by a small rotation (18°) about an axis perpendicular to the DNA helical axis, combined with a 35 Å translation parallel with the DNA helical axis. This matches closely the expected 34 Å distance separating the center of the two TTGC repeats (10 bps at 3.4 Å/bp).

Tetramerization, or dimerization of the A/B and C/D dimers, is achieved through interactions of the C-terminal helices (h4) from each monomer. To accommodate the combined 2-fold symmetry within each dimer of DBDs, and the translational symmetry relating the DBD dimers, each h4 emanates from its DBD at a unique orientation (Figure 2), facilitated by an unstructured linker of four to eight residues (depending on the monomer) connecting h3 with h4. The h4 helices interact in pairs, with the monomer A h4 (A-h4) pairing with B-h4, and C-h4 pairing with D-h4. The two pairs of helices then dimerize into an asymmetric four-helix bundle.

λcII/DNA Interactions

The cII protein binds the DNA as a tetramer (a dimer of dimers), with the A/B dimer interacting with the upstream TTGC and the C/D dimer interacting with the downstream TTGC (Figure 1B). Only one monomer from each dimer (monomers A and C) makes sequence-specific interactions with the DNA TTGC repeats via the recognition helix (h3a), inserted deep within the major groove (Figure 3). The protein makes sequence-specific interactions with every base pair of the two TTGC repeats (monomer A with the upstream repeat, monomer C with the downstream repeat; Figures 3B and 4). The interactions of monomer A with the upstream TTGC motif and monomer C with the downstream TTGC motif are nearly identical (Figure 4). Lys37 and Ser41 make van der Waals interactions with the C5-methyl groups of T_1 and T_2, respectively (where the TTGC motif is represented as $T_1T_2G_3C_4$). Asp36 makes water-mediated hydrogen bonds with N6 and N7 of the A opposite T_2. Arg42 makes hydrogen bonds with both O6 and N7 of G_3. Ser38 hydrogen bonds with N4 of the C opposite G_3. Gln39 makes a hydrogen bond with N7 of the G opposite C_4. Finally, a single water molecule mediates interactions between O6 of the G opposite C_4 and three residues, Ser38, Gln39, and Arg42. These observations are consistent with genetic studies indicating that every base mutated within the two TTGC repeats caused defects in cII binding, while substitutions within the intervening –35 element had no effect (Ho et al., 1983; Shih and Gussin, 1983, 1984).

Mutants of cII with substitutions within the HTH motif, Ser38Leu and Arg42Gly, retained the ability to tetramerize but were unable to bind DNA or activate transcription (Ho et al., 1988). Both of these substitutions would disrupt sequence-specific interactions described above. In addition, the Ser38Leu substitution would introduce a severe steric clash with the DNA.

The 2-fold symmetry within each A/B and C/D dimer positions the recognition helix of monomers B and D to also contribute to DNA interactions, mostly with the DNA phosphate backbone, or through opportunistic interactions with bases outside of the conserved TTGC repeats (Figure 3A). These sequence-specific interactions outside the TTGC repeats may help explain the lack of crossactivation for cII homologs from closely related lambdoid phages (Wulff and Mahoney, 1987).

The helical axis of the DNA interacting with cII bends about 25° (Figure 1B). This bend in the DNA may have functional significance (see below).

Comparison of the cII and cII-DNA Complex

The structures of free and DNA bound cII are very similar, with an rmsd within 1.4 Å when comparing residues

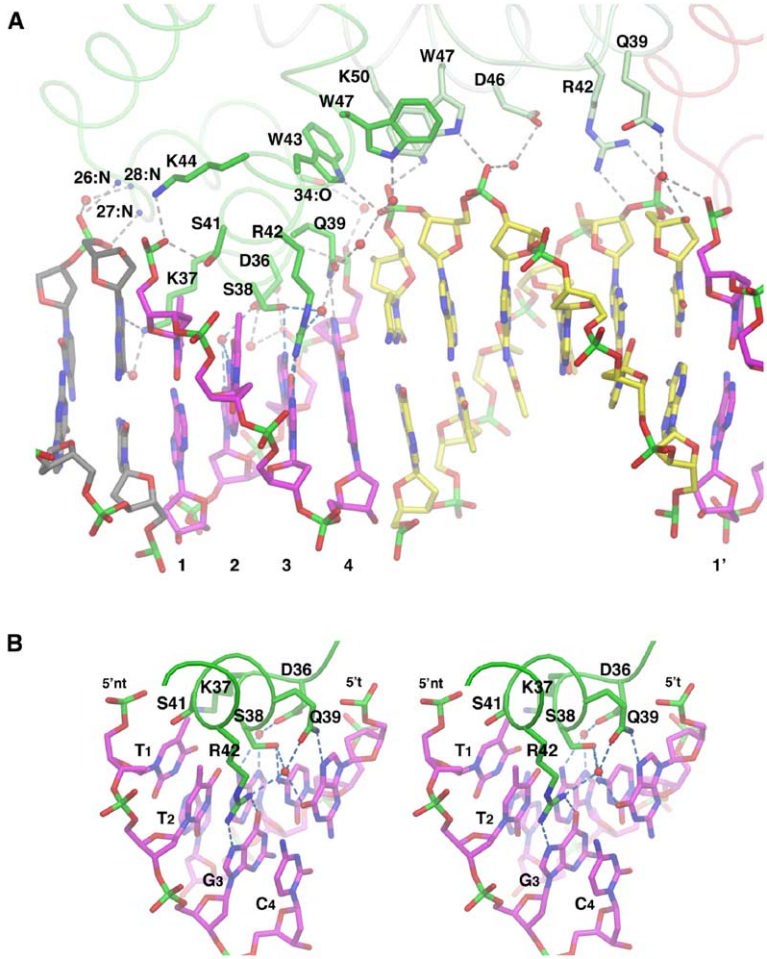

Figure 3. Structure of the λcII/DNA Complex: Protein/DNA Interactions

(A) Overview showing λcII/DNA interactions for monomers A (dark green) and B (light green). The α carbon backbones of the protein chains are shown as transparent worms. Side chains and backbone atoms that contact the DNA are shown. Potential hydrogen bonds (<3.2 Å) are shown as gray dashed lines. Carbon atoms of the side chains are colored as the backbone, nitrogen atoms are blue, and oxygen atoms are red. Water molecules mediating protein/DNA contacts are shown as red spheres. For the DNA, carbon atoms are gray except for the TTGC motifs (magenta) and the –35 element (yellow). The positions of the TTGC motifs are labeled below the DNA (as in Figure 1A).

(B) Stereo view showing protein/DNA interactions between λcII monomer A and the bases of the upstream TTGC motif ($T_1T_2G_3C_4$). The color coding is as in Figure 3A. Only the DNA atoms for the upstream TTGC motif are shown for clarity.

10–58 of each monomer. However, when the entire tetramer is compared, a significant structural difference is revealed, arising from a hinge-like movement of the A/B and C/D dimers with respect to the C-terminal helical bundle (Figure 5). In the DNA bound form, the A/B and C/D dimers are closer to each other—cII is in a relatively closed conformation. The distance from the center of gravity (cog) of the A/B dimer to the C/D cog is about 35 Å, while in the open conformation (cII alone), the distance is about 42 Å. Whether this observation has any functional significance, or is just a crystal packing artifact, is unclear.

Implications for the Activation Mechanism

To provide insight into the cII activation mechanism, we generated a structural model for the λcII/RNAP holoenzyme/promoter DNA complex. First, to position σ_4 with respect to the cII/DNA complex, we superimposed the –35 element DNA from the previously determined structure of the *Thermus aquaticus* (*Taq*) σ_4/–35 element DNA complex (Campbell et al., 2002) onto the –35 element DNA of the cII/DNA complex. Then, we superimposed the so-positioned σ_4 structural core (*Taq* σ_4 residues 376–424; Campbell et al., 2002) with σ_4 from a model of the RNAP holoenzyme open promoter complex (Murakami et al., 2002) and then replaced the open complex model DNA with the corresponding DNA from the cII/DNA complex. In this model, cII does indeed bind to the promoter DNA on the opposite face of the double helix as the RNAP holoenzyme, and there does not appear to be any opportunity for direct protein/protein contacts between cII and any part of the RNAP holoenzyme present in the model, including σ. However, the RNAP αCTDs, which are not present in this model, are known to play a critical role in cII-dependent activation (Gussin et al., 1992; Kedzierska et al., 2004; Marr et al., 2004; Obuchowski et al., 1997a; Wegrzyn et al., 1992).

The *Ec* RNAP α subunits play a key role in RNAP assembly and transcription initiation (Busby and Ebright, 1994; Gourse et al., 2000). Each α subunit consists of two independently folded domains (Blatter et al., 1994; Jeon et al., 1995; Zhang and Darst, 1998). The N-terminal domain (residues 1–235) is essential for assembly of the RNAP core enzyme (Zhang et al., 1999). The αCTD (residues 249–329) is connected to the αNTD by an unstructured, flexible linker of 14 residues (Jeon et al., 1997). The αCTD stimulates transcription initiation by minor-groove binding to AT-rich sequence elements upstream of the –35 element at many promoters (Gourse et al., 2000; Ross et al., 1993), and it is also a direct target for a wide array of transcription activators

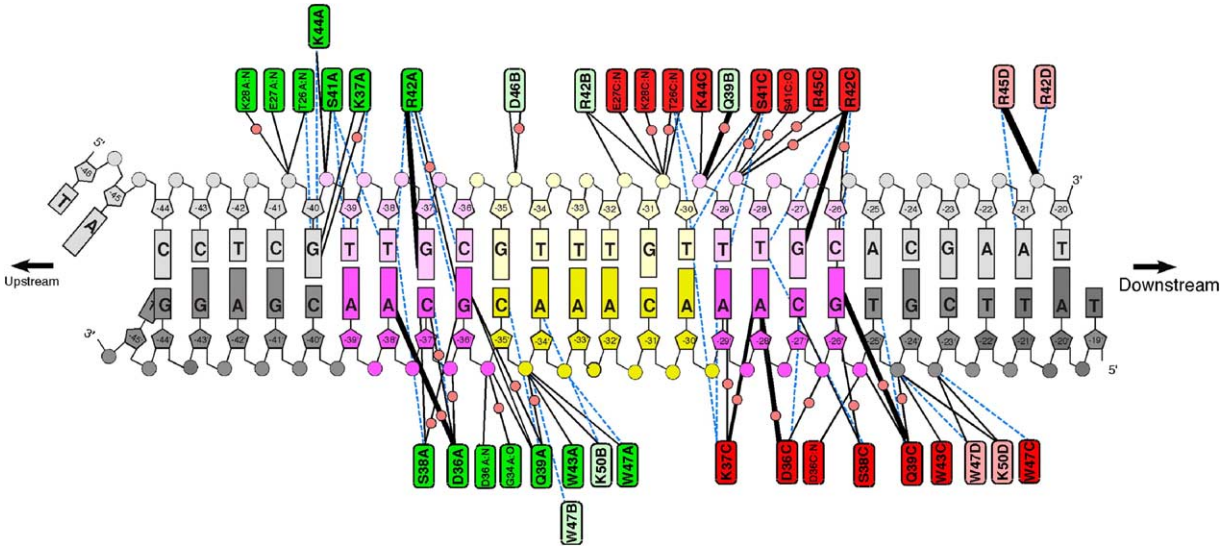

Figure 4. Schematic of λcII/DNA Contacts

Schematic representation of protein/DNA interactions. The DNA is color coded as in Figure 1A. Colored boxes denote protein residues color coded according to λcII monomer as in Figure 1B (dark green, λcIIA; light green, λcIIB; red, λcIIC; and pink, λcIID). Connecting, black solid lines indicate hydrogen bonds (<3.2 Å) or salt bridges (<4 Å) between protein and DNA. Thick solid lines indicate more than one hydrogen bond with the same residue. Water molecules are shown as pink spheres. Van der Waals interactions (<4 Å) are indicated as dashed blue lines.

(Ishihama, 1993). Three separate interaction determinants important for these functions have been identified on αCTD: (1) The 261 determinant, used for interactions of αCTD with the Arg603 determinant of σ_4 when αCTD is positioned just upstream of the –35 element (Chen et al., 2003; Ross et al., 2003; Savery et al., 2002); (2) the 265 determinant, essential for DNA binding (Benoff et al., 2002; Gaal et al., 1996; Murakami et al., 1996); and (3) the 287 determinant, used for interacting with the catabolite activator protein (CAP) at both class I (where αCTD binds between CAP and RNAP) and class II promoters (where CAP binds between αCTD and RNAP; Lawson et al., 2004; Savery et al., 1998, 2002).

In the case of cII-dependent activation at P_{RE}, experiments using RNAP reconstituted with αCTDs derivatized with DNA cleavage reagents showed that one αCTD binds near the –41 position, and alanine-scanning mutagenesis indicated that the 265 determinant was important for full activation (Kedzierska et al., 2004; Marr et al., 2004). These same studies implicated the 261 determinant in cII-dependent activation. Moreover, the substitution Arg603Ala in σ_4 causes λ to form very clear plaques (S.E. Brown and G.N.G., unpublished

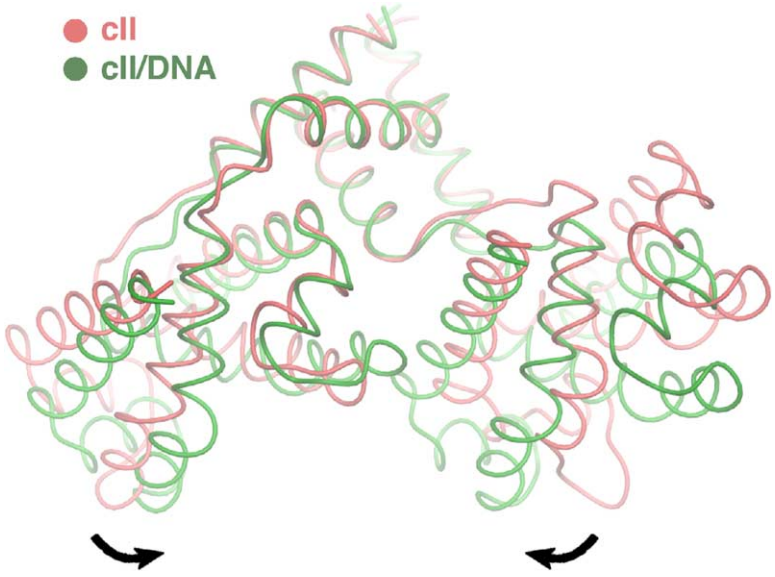

Figure 5. Comparison of cII with and without DNA

The α carbon backbones of cII alone and cII in the cII/DNA complex are shown as worms and color coded as indicated. The structures were superimposed using the C-terminal helices (h4 residues 65–79 for each monomer), with an rmsd over 60 α carbons of 0.86 Å. The arrows indicate the hinge-like motion to move the DBDs from the cII (open) conformation to the cII/DNA (closed) conformation.

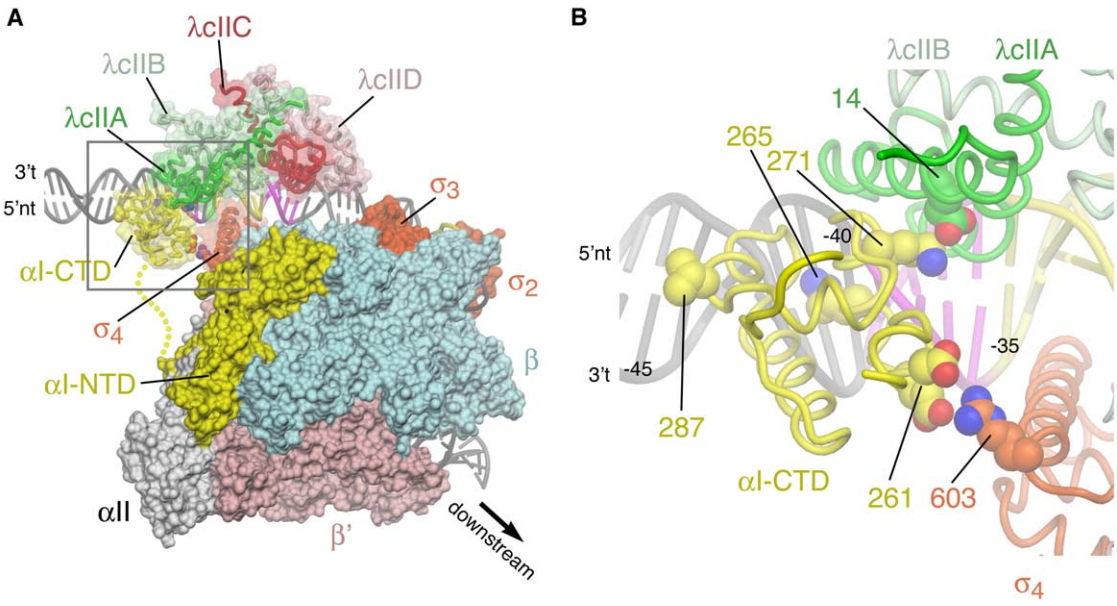

Figure 6. Model of Protein/Protein Interactions in cII Activation

(A) Structural model of the λcII/RNAP holoenzyme open promoter complex. RNAP holoenzyme is shown as a molecular surface, with the σ_4 and αI-CTD surfaces transparent, revealing the backbone worms underneath (only one αCTD is shown). The λcII is also shown as backbone worms with transparent molecular surfaces. Color coding is as follows: αI-NTD and αI-CTD, yellow; αII ω, gray; β, cyan; β′, pink; σ, orange; λcIIA, dark green; λcIIB, light green; λcIIC, red; and λcIID, pink. The linker connecting the αI-NTD with the αI-CTD is shown as a dotted yellow line. The DNA is shown as phosphate backbone worms colored gray, except the cII-specific TTGC motifs are magenta, and the –35 element is yellow. The template (t) and nontemplate (nt) strands are labeled. The boxed region is magnified in (B).

(B) Details of the proposed λcIIA/αI-CTD/σ_4 interactions (similar view as in [A]). Proteins are shown as α carbon backbone worms color coded as follows: λcIIA, dark green; λcIIB, light green; αI-CTD, yellow; and σ_4 orange. Selected side chains are shown as CPK atoms with carbons colored as the protein backbones; nitrogen atoms, blue; and oxygen atoms, red. On λcIIA, Glu14 is shown (putative interaction with αI-CTD Lys271). On αI-CTD, side chains of known determinants are shown and labeled: 261 determinant, Asp259 and Glu261 (interact with σ_4 603 determinant (Chen et al., 2003; Ross et al., 2003; Savery et al., 2002); 265 determinant, Arg265 (essential for DNA binding (Benoff et al., 2002; Gaal et al., 1996; Murakami et al., 1996); and 287 determinant, Val287 (interacts with CAP) (Lawson et al., 2004; Savery et al., 2002; Savery et al., 1998). In addition, Lys271 is shown (putative interaction with λcIIA Glu14). On σ_4, the 603 determinant is shown (*Ec* σ_4 Arg603, corresponding to *Taq* Arg429, important for interacting with αCTD 261 determinant (Chen et al., 2003; Ross et al., 2003; Savery et al., 2002). The DNA is shown as in (A) with the –35, –40, and –45 positions labeled (with respect to the transcription start site).

data). Since, at very low frequency, λ can form stable lysogens in the σ_4-Arg603 mutant strain, σ_4-Arg603 appears to be required for cII-mediated activation of pRE, but not for cI-mediated activation of pRM. These results strongly suggest that an αCTD binds to the DNA just upstream of the –35 element (centered around –41) and uses its 261 determinant to interact with Arg603 of σ_4. To take these findings into account, we incorporated an αCTD into our model. The structure of an αCTD/DNA complex was taken from the αCTD/CAP/DNA structure of Benoff et al. (2002). To position the αCTD in the context of the cII/RNAP holoenzyme/DNA model, the appropriate DNA of the αCTD/DNA structure was superimposed with the DNA from –40 to –42 of the cII/RNAP holoenzyme/DNA model. The resulting model (Figure 6) provides important insights into the activation mechanism of cII.

In the model, the αCTD interacts with the DNA minor groove at around –41, through its 265 determinant. This positions αCTD residues Asp259 and Glu261 (and the rest of the 261 determinant) to interact with Arg603 of *Ec* σ_4 (the 603 determinant; (Chen et al., 2003; Ross et al., 2003), which corresponds to Arg429 of *Taq* σ_4. These structural features were expected from constraints that were used in constructing the model.

The most important insight from the model, which was not a constraint in its construction, is that the placement of αCTD with its 265 determinant interacting with the DNA minor groove at –41, and with the 261 determinant interacting with the 603 determinant of σ_4, positions αCTD in such a way that it could make a protein/protein interaction with the most upstream monomer (monomer A) of cII. Supporting this inference from our model, amino acid substitutions in both cII (Glu14-Lys; Ho et al., 1988) and αCTD (Lys271Glu; Kedzierska et al., 2004; Marr et al., 2004; Wegrzyn et al., 1992) caused defects in cII-mediated activation at P_{RE}. In our model, these two residues are positioned to make a favorable electrostatic interaction. Substitution of either residue with the oppositely charged residues (cII-Glu14Lys or αCTD-Lys271Glu) would cause an unfavorable electrostatic interaction. The substitution αCTD-Lys271Ala has only a minor effect on cII-dependent activation (Kedzierska et al., 2004; Marr et al., 2004), suggesting that the putative αCTD-Lys271/cII-Glu14 electrostatic interaction makes a small contribution to

the overall favorable interaction energy, but that the effect introduced by the αCTD-Lys271Glu substitution tips the balance toward an overall unfavorable interaction. This is consistent with other genetic (reviewed in Busby and Ebright, 1999; Savery et al., 2002) and structural studies of activation (Benoff et al., 2002; Jain et al., 2004), indicating that protein/protein interactions between activators and the RNAP involve very small interfaces of only a few residues, giving rise to only slightly favorable interaction energies.

An additional finding that is consistent with our model came from Wulff and Mahoney (1987), who found that a G to A substitution at position –43 of P_{RE} increased the promoter strength by about a factor of 2. The cII protein does not interact with the DNA at this poisition (Figure 4), but this substitution likely enhances the interaction of αCTD with the DNA. UP elements, the DNA binding target of αCTD, are A/T rich (Ross et al., 1993), and the –43 position of a consensus UP element sequence is A (Estrem et al., 1998, 1999).

Another interesting observation from the model is that the 25° DNA bend of the cII/DNA complex (mentioned above and shown in Figure 1B) is coincident with the DNA bend seen in the σ_4/–35 element DNA structure (Campbell et al., 2002). Assuming that the DNA in this region is not naturally bent, the DNA bend introduced by cII may have a positive effect on the binding of RNAP to the promoter by preforming the –35 element DNA for a favorable interaction with σ_4. This may help explain why truncation of the αCTDs, although causing a severe defect in cII-dependent activation at P_{RE}, did not completely abolish activation in the in vitro study of Gussin et al. (1992). In that study, where the conditions were such that transcription from P_{RE} was totally dependent on cII, the level of transcript produced by αCTD-less RNAP was roughly 20% of the level obtained with wild-type RNAP.

Conclusions

Here, we have presented a high resolution view of the λcII complex with its operator DNA. As expected, the functional unit for cII is a tetramer, although lacking 4-fold symmetry. The DBDs from each monomer pair up to form dimers, while the C-terminal helix from each monomer emanates from the DBD at unique orientations to form an asymmetric four-helix bundle that mediates tetramerization. The HTH motifs of one monomer from each dimer make sequence-specific contacts with the direct repeats of the DNA operator, while the other monomer contributes to DNA binding mostly through phosphate-backbone interactions.

The cII/DNA structure provides a basis for understanding cII-dependent activation. A model of the cII/RNAP holoenzyme/promoter complex indicates that, although the cII-specific direct repeats straddle the promoter –35 element, cII is unlikely to make direct protein/protein interactions with σ_4 bound at the –35 element. Instead, the model points to a key role for the αCTD, which binds the DNA minor groove just upstream of the operator, and makes simultaneous protein/protein interactions with cII (between determinants near cII-Glu14 and αCTD-Lys271) and σ_4 (between the αCTD-261 determinant and the σ_4-603 determinant). In this way, the αCTD serves as a protein bridge, making interactions with the activator cII on one surface, and with the rest of the RNAP through interactions with σ_4 on another. The αCTD-Lys271Glu mutation (*rpoA341* allele, or *phs* mutant) that disrupts cII-dependent activation was the very first mutation identified in αCTD to cause activation defects at a number of positively regulated promoters (Giffard and Booth, 1988). More recent studies have identified αCTD residues 271–273 as a surface-exposed patch that likely serves as the target of the activator Fis (Aiyar et al., 2002; McLeod et al., 2002). However, since Fis binds to sites upstream of the promoter –35 elements on the same face of the DNA duplex as the RNAP, the architecture of the Fis/αCTD/DNA interaction is likely to be similar to architectures described for CAP (Lawson et al., 2004) and very different from the cII/αCTD/DNA architecture proposed here (Figure 6). Finally, binding of cII bends the operator DNA in a way that may enhance the interaction of σ_4 to the –35 element, which may make a minor contribution to the activation effect of cII.

Experimental Procedures

Protein and Nucleic Acid Preparation

Both full-length and truncated (residues 4–82) cII were cloned into the pET15b expression vector (Novagen) and transformed into *E. coli* BL21(DE3) cells. Transformants were grown at 37°C in LB medium supplemented with ampicillin (100 μg/ml) to an A600 of 0.6. Expression was induced by adding 1 mM isopropyl-D-thiogalactopyranoside. After 3 hr, cells were harvested by centrifugation, lysed in a continuous flow French press or by sonication, and clarified by centrifugation. The λcII was purified by Ni^{2+}-affinity chromatography (HiTrap chelating cartridge, Amersham Biotech), followed by thrombin cleavage (100 μg thrombin/100 mg protein) overnight at 4°C, then reapplied to the Ni^{2+}-affinity column. The protein was further purified by gel filtration (Superdex 75, Amersham Biotech). The purified λcII was concentrated to 20 mg/ml by centrifugal filtration (Millipore) and exchanged into 10 mM HEPES (pH 7.5), 150 mM NaCl, and 0.1 mM EDTA. The purified protein was flash frozen and stored at –80°C. Selenomethionyl-substituted λcII was prepared for MAD analysis by suppression of methionine biosynthesis (Doublie, 1997). Purification and crystallization of the selenomethionyl-λcII was identical to wild-type, except buffers included 5 mM dithiothreitol.

Lyophilized, tritylated, single-stranded oligonucleotides (Oligos Etc.) were detritylated and purified as described (Aggarwal, 1990). Dried oligonucleotides were dissolved in 5 mM triethyl ammonium bicarbonate (pH 8.5) to a concentration of 2 mM. Equimolar amounts of complementary oligonucleotides were annealed by heating to 90°C for 5 min and cooling to 22°C at a rate of 0.01°C/s.

Limited Proteolysis, N-Terminal Sequencing, and Mass Spectrometry

Trypsin digests were carried out in 20 mM Tris-HCl (pH 8), 50 mM NaCl, 5% (v/v) glycerol, 0.1mM EDTA. 100 pmoles of λcII were digested in a 10 μl volume with different amounts of trypsin (0.01 pmol – 4.8 pmol) for 30 min at 25°C. Reactions were terminated by the addition of Laemmli loading buffer and boiling. Reaction products were analyzed on denaturing 8%–25% gradient PHAST gels (Pharmacia) followed by Coomassie blue staining. Preparative samples for N-terminal sequencing were separated on 20% Tris-glycine polyacrylamide gels and blotted onto PVDF membrane (Bio-Rad). Fragments were excised and submitted for N-terminal sequence analysis at the protein sequencing facility at the University of Texas Medical Branch, Galveston, TX.

Electrospray mass spectrometry was used to determine the molecular mass of the proteolyzed fragments. Samples were loaded onto Sep-Pak cartridges that were preequilibriated with 0.1%

trifluroacetic acid (TFA). Cartridges were then washed with 5 ml of 0.1% TFA and eluted in 70% acetonitrile..

Crystallization

Complex cocrystals were obtained by vapor diffusion by mixing the duplex DNA and λcII^{4-82} (molar ratio 1.2:1) with the final concentration of DNA at 0.85 nM. The mixture was incubated on ice for 20 min, then 1 μl of this mixture was mixed with 1 μl of 8% PEG550 monomethylether (MME) and incubated at 22°C. SDS-PAGE analysis of the washed, dissolved crystals indicated a binary complex. Crystals were prepared for cryocrystallography by successive transfers into increasing concentrations of PEG550 MME from 10% to 30% in steps of 5%. After the final soak in 30% PEG550 MME, the crystals were flash frozen in a vial of liquid nitrogen. Crystals of full-length, uncomplexed cII were obtained by vapor diffusion in hanging drops over 22% PEG3350, 0.16 M potassium fluoride, For cryocrystallography, the crystals were flash frozen with the crystallization buffer plus 25% ethylene glycol.

Structure Determination

cII^{4-82}/DNA Cocrystals

MAD data were collected at three wavelengths corresponding to the peak, the inflection, and one remote value of the X-ray absorption spectrum (λ1, λ2, and λ3, and, respectively; Table 1) at the National Synchrotron Light Source Beamline X9A (Brookhaven National Laboratory). The data were processed using HKL2000 and SCALEPACK (Otwinowski and Minor, 1997).

Using the anomalous signal from SeMet(λ1), 10 of a possible 12 Se sites in the asymmetric unit were located using SnB (Weeks and Miller, 1999). Phases were calculated using MLPHARE (Otwinowski, 1991). SeMet(λ1) was treated as the reference, and anomalous signals from SeMet(λ1), SeMet(λ2), and SeMet(λ3) gave the best electron density map (2.3 Å resolution). Density modification and phase extension with the Native cII/DNA amplitudes to 1.7 Å resolution using DM (Cowtan, 1994) yielded an excellent map.

The program Arp/Warp (Perrakis et al., 1999) was used to build the protein backbone model into the electron density map, while the DNA was built manually. The side chains were then added manually. Model building was done using O (Jones et al., 1991). The map was improved through iterative cycles of refinement against the native amplitudes, and SIGMAA-weighted phase combination using CNS (Adams et al., 1997). PROCHECK (Laskowski et al., 1993) revealed no residues in disallowed regions of the Ramachandran plot.

Full-Length cII

Data were collected at the wavelength corresponding to the peak energy of the Se X-ray absorption spectrum at the Structural Biology Center Beamline 19ID at the Advanced Photon Source (Argonne National Laboratory) and processed using HKL2000 (Otwinowski and Minor, 1997). The structure soluion was first attempted by molecular replacement using MOLREP (Vagin and Teplyakov, 1997) with the DBD dimer A/B from the cII/DNA structure as the search model with the Native amplitudes. An obvious solution comprising two DBD dimers was found. However, the resulting maps did not allow tracing of the C-terminal helices. Using the anomalous signal from the SeMet(λ1) dataset, the Se sites were located (independent of the molecular replacement phases) using SnB (Weeks and Miller, 1999) and SOLVE (Terwilliger and Berendzen, 1999). The Se sites confirmed the initial molecular replacement solution. SOLVE was used for phasing to 3.5 Å resolution, followed by density modification and phase extension to 2.8 Å using the Native amplitudes with RESOLVE (Terwilliger, 2000). The molecular replacement model was then docked into the electron density map and the residues 60–81 were built manually. The residues beyond 81 could not be traced in any of the cII monomers and are assumed to be disordered. Refinement was carried out with CNS (Adams et al., 1997). Final rounds of refinement were performed using REFMAC (Murshudov et al., 1997), incorporating TLS restraints (Winn et al., 2001) for the cII monomers.

Supplemental Data

Supplemental Data include four figures and can be found with this article online at http://www.molecule.org/cgi/content/full/19/2/259/DC1/.

Acknowledgments

We thank U. Ramagopal at the National Synchrotron Light Source for support at Beamline X9A, and Tom Muir for access to the electrospray mass spectrometer. Figures were generated using DINO (http://www.dino3d.org). D.J. was supported by a Jane Coffin Childs Postdoctoral Fellowship. K.L.M. was supported by a Canadian Institutes of Health Research Postdoctoral Fellowship. Work at the Advanced Photon Source Beamline SBC-19ID was supported by National Institutes of Health grant GM62414 and by the U.S. Department of Energy, Office of Biological and Environmental Research, under contract W-31-109-Eng-38. This work was supported by a Canadian Institute of Health Research grant to A.M.E., and National Institutes of Health grant GM53759 to S.A.D.

Received: April 26, 2005
Revised: June 1, 2005
Accepted: June 7, 2005
Published: July 21, 2005

References

Adams, P.D., Pannu, N.S., Read, R.J., and Brunger, A.T. (1997). Cross-validated maximum likelihood enhances crystallographic simulated annealing refinement. Proc. Natl. Acad. Sci. USA *94*, 5018–5023.

Aggarwal, A.K. (1990). Crystallization of DNA binding proteins with oligodeoxynucleotides. Methods *1*, 83–90.

Aiyar, S.E., McLeod, S.M., Ross, W., Hirvonen, C.A., Thomas, M.S., Johnson, R.C., and Gourse, R.L. (2002). Architecture of Fis-activated transcription complexes at the *Escherichia coli rrnB* P1 and *rrnE* P1 promoters. J. Mol. Biol. *316*, 501–516.

Beamer, L.J., and Pabo, C.O. (1992). Refined 1.8 Å crystal structure of the l repressor-operator complex. J. Mol. Biol. *227*, 177–196.

Benoff, B., Yang, H., Lawson, C.L., Parkinson, G., Liu, J., Blatter, E., Ebright, Y.W., Berman, H.M., and Ebright, R.H. (2002). Structural basis of transcription activation: The CAP-aCTD-DNA complex. Science *297*, 1562–1566.

Blatter, E., Ross, W., Tang, H., Gourse, R., and Ebright, R. (1994). Domain organization of RNA polymerase slpha subunit: C-terminal 85 amino acids constitute a domain capable of dimerization and DNA binding. Cell *78*, 889–896.

Busby, S., and Ebright, R.H. (1994). Promoter structure, promoter recognition, and transcription activation in prokaryotes. Cell *79*, 743–746.

Busby, S., and Ebright, R.H. (1999). Transcription activation by catabolite activator protein (CAP). J. Mol. Biol. *293*, 199–213.

Campbell, E.A., Muzzin, O., Chlenov, M., Sun, J.L., Olson, C.A., Weinman, O., Trester-Zedlitz, M.L., and Darst, S.A. (2002). Structure of the bacterial RNA polymerase promoter specificity sigma factor. Mol. Cell *9*, 527–539.

Chen, H., Tang, H., and Ebright, R.H. (2003). Functional interaction between RNA polymerase α subunit C-terminal domain and σ70 in UP-element- and activator-dependent transcription. Mol. Cell *11*, 1621–1633.

Cowtan, K. (1994). Dm-density modification package. ESF/CCP4 Newsletter *31*, 34–38.

Datta, A.B., Roy, S., and Parrack, P. (2005). Role of C-terminal residues in oligomerization and stability of l CII: Implications for lysis-lysogeny decision of the phage. J. Mol. Biol. *345*, 315–324.

Doublie, S. (1997). Preparation of selenomethionyl proteins for phase determination. Methods Enzymol. *276*, 523–530.

Dove, S.L., Darst, S.A., and Hochschild, A. (2003). Region 4 of sigma as a target for transcription regulation. Mol. Microbiol. *48*, 863–874.

Echols, H. (1986). Bacteriophage l development: Temporal switches and the choice of lysis or lysogeny. Trends Genet. *2*, 26–30.

Estrem, S.T., Gaal, T., Ross, W., and Gourse, R.L. (1998). Identification of an UP element consensus sequence for bacterial promoters. Proc. Natl. Acad. Sci. USA *95*, 9761–9766.

Estrem, S.T., Ross, W., Gaal, T., Chen, Z.W.S., Niu, W., Ebright, R.H., and Gourse, R.L. (1999). Bacterial promoter architecture: Subsite structure of UP elements and interactions with the carboxy-terminal domain of the RNA polymerase alpha subunit. Genes Dev. *13*, 2134–2147.

Gaal, T., Ross, W., Blatter, E.E., Tang, H., Jia, X., Krishnan, V.V., Assa-Munt, N., Ebright, R.H., and Gourse, R.L. (1996). DNA-binding determinants of the alpha subunit of RNA polymerase: Novel DNA-binding domain architecture. Genes Dev. *10*, 16–26.

Giffard, P.M., and Booth, I.R. (1988). The rpoA341 allele of *Escherichia coli* specifically impairs the transcription of a group of positively-regulated operons. Mol. Gen. Genet. *214*, 148–152.

Gourse, R.L., Ross, W., and Gaal, T. (2000). UPs and downs in bacterial transcription initiation: The role of the alpha subunit of RNA polymerase in promoter recognition. Mol. Microbiol. *37*, 687–695.

Gussin, G.N., Olson, C., Igarashi, K., and Ishihama, A. (1992). Activation defects caused by mutations in *Escherichia coli rpoA* are promoter specific. J. Bacteriol. *174*, 5156–5160.

Hendrickson, W.A. (1991). Determination of macromolecular structures from anomalous diffraction of synchrotron radiation. Science *254*, 51–58.

Ho, Y.-S., Lewis, M., and Rosenberg, M. (1982). Purification and properties of a transcriptional activator. The cII protein of phage l. J. Biol. Chem. *257*, 9128–9134.

Ho, Y.-S., Wulff, D., and Rosenberg, M. (1986). Protein-nucleic acid interactions involved in transcription activation by the phage lambda regulatory protein cII. In Regulation of Gene Expression—25 Years On, I.R. Booth and C.F. Higgins, eds. (Cambridge: Cambridge University Press), pp. 79–103.

Ho, Y.-S., Wulff, D.L., and Rosenberg, M. (1983). Bacteriophage l protein cII binds promoters on the opposite face of the DNA helix from RNA polymerase. Nature *304*, 703–708.

Ho, Y.S., Mahoney, M.E., Wulff, D.L., and Rosenberg, M. (1988). Identification of the DNA binding domain of the phage l cII transcriptional activator and the direct correlation of cII protein stability with its oligomeric forms. Genes Dev. *2*, 184–195.

Hochschild, A., and Dove, S.L. (1998). Protein-protein contacts that activate and repress prokaryotic transcription. Cell *92*, 597–600.

Ishihama, A. (1992). Role of the RNA polymerase a subunit in transcription activation. Mol. Microbiol. *6*, 3283–3288.

Ishihama, A. (1993). Protein-protein communication within the transcription apparatus. J. Bacteriol. *175*, 2483–2489.

Jain, D., Nickels, B.E., Sun, L., Hochschild, A., and Darst, S.A. (2004). Structure of a ternary transcription activation complex. Mol. Cell *13*, 45–53.

Jeon, Y.H., Negishi, T., Shirakawa, M., Yamazaki, T., Fujita, N., Ishihama, A., and Kyogoku, Y. (1995). Solution structure of the activator contact domain of the RNA polymerase a subunit. Science *270*, 1495–1497.

Jeon, Y.H., Yamazaki, T., Otomo, T., Ishihama, A., and Kyogoku, Y. (1997). Flexible linker in the RNA polymerase alpha subunit facilitates the independent motion of the C-terminal activator contact domain. J. Mol. Biol. *267*, 953–962.

Jones, T.A., Zou, J.-Y., Cowan, S., and Kjeldgaard, M. (1991). Improved methods for building protein models in electron denstiy maps and the location of errors in these models. Acta Crystallogr. *A47*, 110–119.

Karata, K., Inagawa, T., Wilkinson, A.J., Tatsuta, T., and Ogura, T. (1999). Dissecting the role of a conserved motif (the second region of homology) in the AAA family of ATPases. Site-directed mutagenesis of the ATP-dependent protease FtsH. J. Biol. Chem. *274*, 26225–26232.

Kedzierska, B., Lee, D.J., Wegrzyn, G., Busby, S.J., and Thomas, M.S. (2004). Role of the RNA polymerase alpha subunits in cII-dependent activation of the bacteriophage lambda pE promoter: Identification of important residues and positioning of the alpha C-terminal domains. Nucleic Acids Res. *32*, 834–841.

Kobiler, O., Koby, S., Teff, D., Court, D., and Oppenheim, A.B. (2002). The phage l CII transcriptional activator carries a C-terminal domain signaling for rapid proteolysis. Proc. Natl. Acad. Sci. USA *99*, 14964–14969.

Laskowski, R.A., MacArthur, M.W., Moss, D.S., and Thornton, J.M. (1993). PROCHECK—A program to check the stereochemical quality of protein structures. J. Appl. Crystallogr. *26*, 283–291.

Lawson, C.L., Swigon, D., Murakami, K.S., Darst, S.A., Berman, H.M., and Ebright, R.H. (2004). Catabolite activator protein: DNA binding and transcription activation. Curr. Opin. Struct. Biol. *14*, 10–20.

Marr, M.T., Roberts, J.W., Brown, S.E., Klee, M., and Gussin, G.N. (2004). Interactions among CII protein, RNA polymerase and the lambda PRE promoter: Contacts between RNA polymerase and the -35 region of PRE are identical in the presence and absence of CII protein. Nucleic Acids Res. *32*, 1083–1090.

Matthews, B.W., Ohlendorf, D.H., Anderson, W.F., and Takeda, Y. (1982). Structure of the DNA-binding region of the lac repressor inferred from its homology with cro repressor. Proc. Natl. Acad. Sci. USA *79*, 1428–1432.

McLeod, S.M., Aiyar, S.E., Gourse, R.L., and Johnson, R.C. (2002). The C-terminal domains of the RNA polymerase a subunits: Contact site with Fis and localization during co-activation with CRP at the *Escherichia coli proP* P2 promoter. J. Mol. Biol. *316*, 517–529.

Murakami, K., Fujita, N., and Ishihama, A. (1996). Transcription factor recognition surface on the RNA polymerase alpha subunit is involved in contact with the DNA enhancer element. EMBO J. *15*, 4358–4367.

Murakami, K., Masuda, S., Campbell, E.A., Muzzin, O., and Darst, S.A. (2002). Structural basis of transcription initiation: An RNA polymerase holoenzyme/DNA complex. Science *296*, 1285–1290.

Murshudov, G.N., Vagin, A.A., and Dodson, E.J. (1997). Refinement of macromolecular structures by the maximum-likelihood method. Acta Crystallogr. D Biol. Crystallogr. *D53*, 240–255.

Obuchowski, M., Giladi, H., Koby, S., Szalewska-Palasz, A., Wegrzyn, A., Oppenheim, A.B., Thomas, M.S., and Wegrzyn, G. (1997a). Impaired lysogenisation of the *Escherichia coli rpoA341* mutant by bacteriophage l is due to the inability of CII to act as a transcriptional activator. Mol. Gen. Genet. *254*, 304–311.

Obuchowski, M., Shotland, Y., Koby, S., Giladi, H., Gabig, M., Wegrzyn, G., and Oppenheim, A.B. (1997b). Stability of CII is a key element in the cold stress response of bacteriophage lambda infection. J. Bacteriol. *179*, 5987–5991.

Otwinowski, Z. (1991). Maximum likelihood refinement of heavy-atom parameters. In Isomorphous Replacement and Anomalous Scattering, Proceedings of the CCP4 Study Weekend, W. Wolf, P.R. Evans, and A.G.W. Leslie, eds. (UK: Warrington), pp. 80–86.

Otwinowski, Z., and Minor, W. (1997). Processing of X-ray diffraction data collected in oscillation mode. Methods Enzymol. *276*, 307–326.

Pabo, C.O., and Sauer, R.T. (1984). Protein-DNA recognition. Annu. Rev. Biochem. *53*, 293–321.

Perrakis, A., Morris, R., and Lamzin, V.S. (1999). Automated protein model building combined with iterative structure refinement. Nat. Struct. Biol. *6*, 458–463.

Ross, W., Gosink, K., Salomon, J., Igarashi, K., Zou, C., Ishihama, A., Severinov, K., and Gourse, R.L. (1993). A third recognition element in bacterial promoters: DNA binding by the alpha subunit of RNA polymerase. Science *262*, 1407–1413.

Ross, W., Schneider, D.A., Paul, B.J., Mertens, A., and Gourse, R.L. (2003). An intersubunit contact stimulating transcription initiation by *E. coli* RNA polymerase: Interaction of the a C-terminal domain and s region 4. Genes Dev. *17*, 1293–1307.

Savery, N.J., Lloyd, G.S., Busby, S.J.W., Thomas, M.S., Ebright, R.H., and Gourse, R.L. (2002). Determinants of the C-terminal domain of the *Escherichia coli* RNA polymerase a subunit important for transcription at class I cyclic AMP receptor protein-dependent promoters. J. Bacteriol. *184*, 2273–2280.

Savery, N.J., Lloyd, G.S., Kainz, M., Gaal, T., Ross, W., Ebright, R.H., Gourse, R.L., and Busby, S.J.W. (1998). Transcription activation at class II CRP-dependent promoters: Identification of determinants

in the C-terminal domain of the RNA polymerase alpha subunit. EMBO J. *17*, 3439–3447.

Shih, M.-C., and Gussin, G.N. (1983). Differential effects of mutations on discrete steps in transcription initiation at the l P_{RE} promoter. Cell *34*, 941–949.

Shih, M.-C., and Gussin, G.N. (1984). Kinetic effects of mutations affecting the cII activation site of the P_{RE} promoter of bacteriophage l. Proc. Natl. Acad. Sci. USA *81*, 6432–6436.

Tan, S., Hunziker, Y., Pellegrini, L., and Richmond, T.J. (2000). Crystallization of the yeast MATalpha2/MCM1/DNA ternary complex: General methods and principles for protein/DNA cocrystallization. J. Mol. Biol. *297*, 947–959.

Terwilliger, T.C. (2000). Maximum likelihood density modification. Acta Crystallogr. D Biol. Crystallogr. *D56*, 965–972.

Terwilliger, T.C., and Berendzen, J. (1999). Automated MAD and MIR structure solution. Acta Crystallogr. D Biol. Crystallogr. *D55*, 849–861.

Vagin, A., and Teplyakov, A. (1997). MOLREP: An automated program for molecular replacement. J. Appl. Crystallogr. *30*, 1022–1025.

Weeks, C.M., and Miller, R. (1999). The design and implementation of SnB v2.0. J. Appl. Crystallogr. *32*, 120–124.

Wegrzyn, G., Glass, R.E., and Thomas, M.S. (1992). Involvement of the a subunit of *E. coli* RNA polymerase in transcriptional activation by the bacteriophage l regulatory proteins CI and CII. Gene *122*, 1–7.

Winn, M.D., Isupov, M.N., and Murshudov, G.N. (2001). Use of TLS parameters to model anisotropic displacements in macromolecular refinement. Acta Crystallogr. D Biol. Crystallogr. *D57*, 122–133.

Wulff, D.L., and Mahoney, M.E. (1987). Cross-specificities between *cII*-like proteins and p_{RE}-like promoters of lambdoid bacteriophages. Genetics *115*, 597–604.

Zhang, G., Campbell, E.A., Minakhin, L., Richter, C., Severinov, K., and Darst, S.A. (1999). Crystal structure of *Thermus aquaticus* core RNA polymerase at 3.3 Å resolution. Cell *98*, 811–824.

Zhang, G., and Darst, S.A. (1998). Structure of the *Escherichia coli* RNA polymerase α subunit amino-terminal domain. Science *281*, 262–266.

Accession Numbers

Structure coordinates and structure factors from the λcII and λcII/DNA crystals have been deposited in the Protein Data Bank under ID codes 1ZPQ and 1ZS4, respectively.